

# Application of light-emitting diodes for aerosol fluorescence detection

Yong-Le Pan, Véronique Boutou,\* and Richard K. Chang

Department of Applied Physics and Center for Laser Diagnostics, Yale University, New Haven, Connecticut 06520-8284

Ilker Ozden, Kristina Davitt, and Arto V. Nurmikko

Division of Engineering, Brown University, Providence, Rhode Island 02912

Received April 14, 2003

We demonstrate a proof-of-concept optical spectroscopic system for bioaerosol-particle fluorescence detection, in which a pulsed high-power laser is replaced by a highly compact linear array of sequentially fired light from blue light-emitting diodes. The results suggest that low-cost, compact optical aerosol detection may be feasible with the contemporary emergence of efficient UV light-emitting diodes. © 2003 Optical Society of America

OCIS codes: 170.6280, 010.1100, 220.4840.

Ultraviolet laser-induced fluorescence spectroscopy is a useful tool for classifying and discriminating, in real time and *in situ*, bioaerosols from environmental aerosols and nonbioaerosols, and it offers a means for constructing an early-warning system for hazardous airborne materials.<sup>1–5</sup> Because bioaerosols of interest typically exist in small concentrations against a dominant background, a small number of bioaerosol particles must be detected in the presence of a very large concentration of nonbioaerosol particles. Most approaches to date use pulsed high-power solid-state lasers, such as a frequency-quadrupled Nd:YAG laser at 266 nm.<sup>1,3–5</sup> To miniaturize a laser-induced fluorescence system, a microchip Nd:YAG laser has been used.<sup>5</sup> However, an UV semiconductor light-emitting diode (LED) allows further miniaturization. There is intense ongoing research activity to develop efficient UV LEDs for many uses. In applications directed at bioaerosol detection, a question arises: Can such incoherent devices be a practical source for LED-induced fluorescence (LEDIF)? In addition, the fluorescence saturation effects<sup>6</sup> caused by a high-power laser can be avoided with LEDs. Here we suggest that a particular configuration composed of a linear array of LEDs can present a feasible optical engineering choice for the fluorescence-based detection of single flowing aerosol particles. In this Letter we present proof of a concept that employs an array of blue GaN-based LEDs near 470 nm, which provides the approximate output powers and electrical-to-optical efficiencies that can be expected from the nitride UV LEDs that specifically emit near the 280–340-nm wavelength range for optimal fluorescence excitation of tryptophan, NADH, and other key biomolecules.

Our scheme employs a 32-element linear array of blue LEDs, each equipped with a microlens. The devices are fired sequentially in pulsed operation on a submicrosecond time scale as a bioaerosol particle travels along the focal line that is defined by the spatially integrated emission from the LEDs. In this manner, the individual peak intensity from each LED

can exceed its cw intensity. The time-integrated photoexcitation imparted to the particle in the illuminating volume is sufficient for single aerosol detection with LEDIF.

The LEDs were fabricated from standard InGaN/GaN quantum-well *p-h*-junction heterostructure wafers, grown epitaxially on sapphire substrates, with layering designs typical of high-brightness blue LEDs.<sup>7</sup> The devices were fabricated so that the optical output was obtained through a transparent aperture atop the top *p* contact. Indium tin oxide or a *p++/n++* InGaN/GaN tunnel junction was used as a transparent hole current-spreading layer for the necessary emission uniformity across the devices. Some fabrication details can be found in Ref. 8. Each LED had an aperture of 70  $\mu\text{m}$  with a center-to-center distance of 100  $\mu\text{m}$ . A planar electrode configuration allowed each LED to be individually electrically addressable. To improve light extraction and collimation from the devices, each LED was equipped with its own microlens. The microlenses were produced directly on the LEDs by photolithography and the well-known reflow technique (see inset in Fig. 1). As a material for

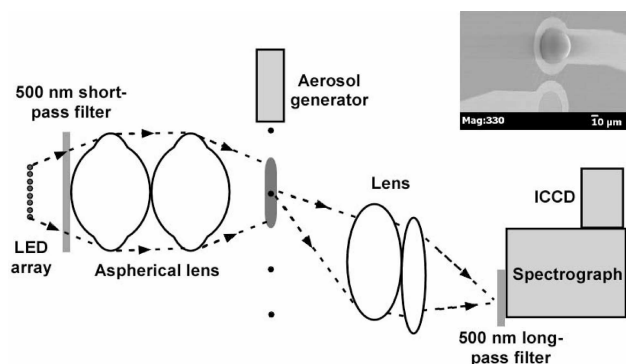


Fig. 1. Schematic of the experimental setup used for detecting LEDIF spectra from individual flowing micrometer-sized aerosol particles. Inset, scanning electron microscopy image from one LED with its microlens.

the visible wavelengths involved here, we used Shipley STR-1075 photoresist for convenience. However, the method is also applicable to UV-transparent epoxies. Typically, we fabricated microlenses with an 80- $\mu\text{m}$  diameter and measured focal lengths of approximately 80  $\mu\text{m}$  for optimizing key light extraction and optical throughput parameters.

The overall experimental arrangement is shown in Fig. 1. The LED array was mounted vertically so that it would be parallel with the straight trajectory of the flowing aerosols. The microlenses provided the first stage in the collection optics. The second stage for collection and imaging was composed of a pair of aspherical lenses ( $f = 12$  mm; F#, 0.68). We estimate that the presence of the microlenses improves the throughput from the LEDs by at least 1 order of magnitude compared with planar devices. The pair of aspherical lenses provided imaging of the LED array output at a sufficient distance from the particle flow so as not to perturb air dynamics and trigger turbulence of the associate particle stream. The overall optical system created a vertical slit of illumination of 300  $\mu\text{m}$  in width and  $\sim 3.2$  mm in length at the focal plane, which coincides with the particle trajectory. Narrower illumination stripe widths are possible as well. The illuminated length is within the focal region of the particles in the laminar stream ( $\sim 3$  cm) of air flowing at 1–10 ms/s produced by our nozzle–injector. The individual LEDs were driven to peak optical powers typically of  $\sim 1$  mW delivered at the jet stream. We note that wall plug efficiencies of the order of 20% have been reached in high-power blue LEDs that have the benefit of sophisticated light extraction and packaging for effective heat sinking.<sup>7</sup> Our devices were experimental test structures where such optimization was not undertaken; rather, the goal was to employ milliwatt-level output power as a reference level in our proof-of-concept experiment in anticipation of comparable performance from the UV LEDs currently under development. For repetitive events, duty cycles as high as several percent were used without adverse device heating effects in the LEDs.

For testing the LEDIF concept with blue excitation, we chose the common biological primary fluorophore riboflavin (RBF) as the test material. The bioaerosols were 50- $\mu\text{m}$  water droplets containing a 0.02% concentration of RBF, which is equivalent to 3- $\mu\text{m}$  solid riboflavin aerosol particles. The monodisperse water droplets were produced by a piezo-driven aerosol generator, which could provide precise synchronization for the electrical pulse driver of the LED array, as well as the gate signal of the ICCD camera (an image-intensified CCD). The duration of the electrical drive pulses for each LED was slightly longer than the fly-by time of the aerosol particle for one emitter ( $\sim 35$   $\mu\text{s}$  versus 30  $\mu\text{s}$ ) so that effectively continuous-wave photoexcitation of  $\sim 1$  ms was ensured in the optical sampling column. The fluorescence from the RBF-doped droplets was collected by one spherical lens (F#, 1.2) and focused by another spherical lens (F#, 3.5) onto the spectrograph slit (1 mm, 300 grooves/mm), before the dispersed spectrum detection by the ICCD.

One potential challenge with any LEDIF-based system is the presence of the long wavelength tails in the LED emission spectrum. (This is more pronounced in green and blue for the nitride emitters than for UV because of the effect of the indium-concentration-related disorder on the conduction and valence-band density of states.) We employed a conventional 500-nm short-pass filter immediately after the LED illumination side and a 500-nm long-pass filter at the spectrometer collection side, as shown in Fig. 2. Use of the short-pass filter (SP) and the long-pass filter (LP) is designated as (SP,LP) when the short-pass filter is placed at the LED illumination side and the long-pass filter is placed at the collection side; it is designated as (0,0) when neither of the two filters is used. Both filters have extinction ratios greater than 1000:1. We note that considerable improvement can be expected if multilayer filters directly deposited on the LEDs or alternatively if spectrally purer resonant cavity emitters are used.<sup>9</sup> To illustrate this point, Fig. 2(a) shows a single LED emission profile (0,0), the accumulated scattering leakage spectrum through a 500-nm long-pass filter from 100 50- $\mu\text{m}$  water droplets (0,LP), and the fluorescence spectrum with the scattering leakage through a 500-nm long-pass filter from 100 50- $\mu\text{m}$  RBF-doped water droplets (0,LP). The subtraction between the two spectra gives the fluorescence spectrum of RBF (solid curve) displayed in Fig. 2(b), thereby illustrating a convenient and fast signal-processing solution to the

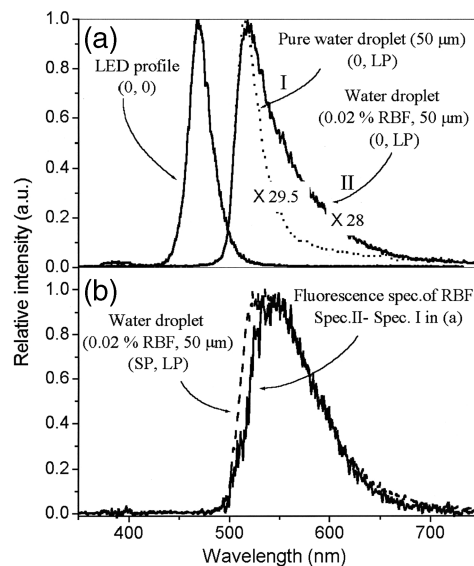


Fig. 2. (a) Single LED emission profile (0,0), the accumulated scattering leakage spectrum (0,LP) through a 500-nm long-pass filter from 100 50- $\mu\text{m}$  pure water droplets, and the fluorescence spectrum with the scattering leakage (0,LP) through a 500-nm long-pass filter from 100 50- $\mu\text{m}$  RBF-doped water droplets. (b) Fluorescence spectrum of a RBF droplet (solid curve) obtained by subtracting spectrum I from spectrum II in (a) and the fluorescence spectrum of a RBF-doped water droplet (dashed curve) (SP,LP) by direct measurement with both the short- and long-pass filters on. The notation in parentheses indicates whether the short-pass (SP) and long-pass (LP) filters were used.

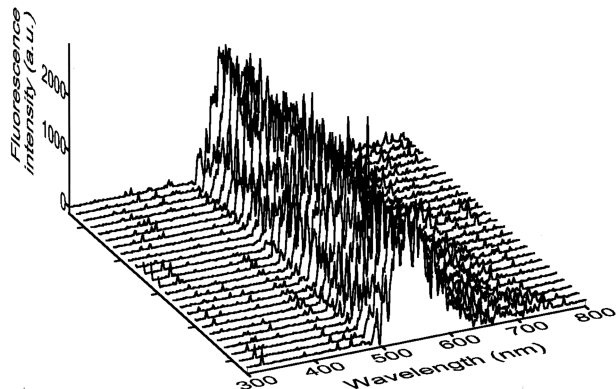


Fig. 3. Twenty-five successive fluorescence spectra from single flowing RBF droplets excited by sequentially emitting the LED array. The LEDs emit in groups of six, starting with 1–6, then 5–10, 9–14, and so on until LEDs 27–32 emit. The ten groups of LEDs run at  $\sim 7000$  Hz to match the flowing speed of the droplet. With this timing condition two LEDs in each group are on for as long as twice the time of the other LEDs. The total fluorescence collection time is  $\sim 1$  ms, which equals one emission cycle of the whole LED array.

combined contribution of the long wavelength tails in the LED emission and scattering from the main spectral features of the LED by the aerosol particles. When the short-pass filter is added (SP, LP), the spectrum from the RBF-doped water droplets is much closer to the pure fluorescence spectrum of RBF itself [see Fig. 2(b), dashed curve]. This implies that a short-pass filter is needed to cut off the long wavelength tail of the LED emission.

Figure 3 illustrates the performance of the whole optical system by displaying 25 successive fluorescence spectra from single flowing RBF droplets excited by a sequentially grouped illuminating mode of the 32-LED array. The temporal gating of the individual LEDs reduces the background scattering (contrasted with the operation in the continuous-wave mode of Fig. 2), and these spectra consistently show good signal-to-noise ratios that demonstrate how the fluorescence spectrum from single micro-sized bioaerosols is detectable via the LED's illumination in the experimental conditions described in this Letter.

In summary, we have demonstrated a technique that shows promise for the detection of bioaerosols by fu-

ture UV LEDs. As a strategy, the use of a linear array of small-aperture LEDs compensates for the lack of their individual brightness when compared with the high-power pulsed UV laser point-excitation configuration. Considerable further improvement is possible with the proof-of-concept scheme discussed above, including miniaturization of the imaging and collection optics and the spectrometer–detector system.

The authors thank M. Krames at Lumileds LLC for providing the epitaxial material for the blue LED fabrication. The work was supported by the Defense Advanced Research Projects Agency's Semiconductor Ultraviolet Optical Sources program under the Space and Naval Warfare Systems Command Systems Center contract N66001-02-C-8017. Y. Pan's e-mail address is yongle.pan@yale.edu.

\*Permanent address, LASIM (Laboratory of Molecular and Ionic Spectroscopy, UMR CNRS 5579), Université Claude Bernard Lyons 1, 43 Boulevard du 11 Novembre 1918, 69622 Villeurbanne Cédex, France.

## References

1. Y. L. Pan, S. Holler, R. K. Chang, S. C. Hill, R. G. Pinnick, S. Niles, and J. R. Bottiger, *Opt. Lett.* **24**, 116 (1999).
2. P. P. Hairston, J. Ho, and F. R. Quant, *Aerosol Sci. Technol.* **28**, 471 (1997).
3. P. H. Kaye, J. E. Barton, E. Hirst, and J. M. Clark, *Appl. Opt.* **39**, 3738 (2000).
4. J. D. Eversole, J. J. Hardgrove, W. K. Cary, Jr., D. P. Choulas, and M. Seaver, *Field Anal. Chem. Tech.* **3**, 249 (1999).
5. F. L. Reys, T. H. Jeys, N. R. Newbury, C. A. Primmerman, G. S. Rowe, and A. Sanchez, *Field Anal. Chem. Tech.* **3**, 240 (1999).
6. S. C. Hill, R. G. Pinnick, S. Niles, N. F. Fell, Jr., Y. L. Pan, J. Bottiger, S. Holler, and R. K. Chang, *Appl. Opt.* **40**, 3005 (2001).
7. J. J. Wierer, D. A. Steigerwald, M. R. Krames, J. J. O'Shea, M. J. Ludowise, G. Christenson, Y.-C. Shen, C. Lowery, P. S. Martin, S. Subramanya, W. Goetz, N. F. Gardner, R. S. Kern, and S. A. Stockman, *Appl. Phys. Lett.* **78**, 3379 (2001).
8. I. Ozden, M. Diagne, A. V. Nurmikko, J. Han, and T. Takeuchi, *Phys. Status Solidi A* **188**, 139 (2001).
9. M. Diagne, Y. He, H. Zhou, E. Makarona, A. V. Nurmikko, J. Han, K. E. Waldrip, J. J. Figiel, T. Takeuchi, and M. Krames, *Appl. Phys. Lett.* **79**, 3720 (2001).